Microelectronics Journal 45 (2014) 508–514

Contents lists available at ScienceDirect

Microelectronics Journal

journal homepage: www.elsevier.com/locate/mejo

Investigation of the thermal properties of thin solid materials at different temperature levels using a set of microresistors

Ali Assy [a,b,d,*], Séverine Gomès [a,b,d], Patrice Chantrenne [a,c,d], Nicolas Pavy [e], Jayalakshmi Parasuraman [e], Xavier Kleber [a,c,d], Philippe Basset [e]

[a] Université de Lyon, France
[b] Bâtiment Sadi Carnot, 9 rue de la physique, INSA de Lyon, 69621 Villeurbanne Cedex, France
[c] Bâtiment B. Pascal, 7 Avenue Jean Capelle 69621 Villeurbanne cedex, France
[d] INSA de Lyon, Lyon F-69621, France
[e] Bâtiment Copernic, 5 bd Descartes, Champs-sur-Marne, 77454 Marne-la-Vallée Cedex 2, France

ARTICLE INFO

Article history:
Received 29 November 2012
Received in revised form
4 August 2013
Accepted 8 August 2013
Available online 12 September 2013

Keywords:
Thermal diffusivity
Thermal conductivity
Contact metrology
Microresistors

ABSTRACT

The measurement of thermal properties of solid materials at different temperatures above ambient is investigated using a set of microresistors. Samples consisted of suspended films with sets of long, parallel resistive wires deposited on their surfaces. One resistive wire was heated by an alternating current. Surface temperature changes in DC and AC regimes were then detected by measuring the change in electrical resistance of the other wires deposited on the surface. The length of wires was chosen so that they may be assumed isothermal and such that heat diffusion acts perpendicularly to their axes. By measuring the dependence of the surface alternating temperature oscillation on the modulation frequency f and on the separation between the heating wire and the probing wires, the thermal diffusivity of the sample was determined. Through adjustment of the alternating current amplitude in the source wire, the temperature at which the thermal diffusivity of the sample was evaluated was finely controlled. For the validation of the method, pure silicon samples were first studied. An experimental bench was set up and resistive source and probes were experimentally characterized. Results obtained from ambient temperature to 500 K for pure silicon are in accordance with reference data found in the scientific literature.

1. Introduction

Characterization of the thermal diffusivity and conductivity of bulk materials and thin films is very important in various application domains (microelectronic, nuclear, materials for aeronautics…). To achieve such a determination, different methods have been developed. They can be classed in two main groups, the non-contact optical methods, also called photothermal methods and the contact methods using contact electrical means.

For the non-contact methods, the thermal source is usually photothermally created. In many cases, the sample is illuminated by a pump modulated laser beam. This laser causes heating of the sample through absorption and subsequent thermalization of energy. By covering the surface with a thin layer that is optically thick at the wavelength of the light, the heating at the sample surface is localized. A spot, a straight line or a domain of the surface can be illuminated. They correspond respectively to cylindrical, plane, and 1D propagation regimes of thermal waves. The analysis of the temperature of the sample surface as a function of the modulation frequency of the thermal source or the distance to the thermal source allows the determination of the sample thermal properties. Pulsed heating sources are used also as in the flash method [1,2]. Through numerous detection schemes available nowadays such as mirage setup [3,4], photoreflectance microscopy [5–8] or photothermal radiometry [9,10], the variations of the surface temperature are measured. Thermal parameters are then extracted from fitting these measurements with curves calculated with the model of heat spreading in the sample.

Considering now the thermal methods using contact electrical means, various methods discussed in Ref. [11] are based on the transient hot strip source technique proposed by Gustafsson [12] and the 3ω method of Cahill [13]. Both methods were initially developed for measuring the thermal conductivity of bulk materials. In these methods, the sample is heated by a thin metal strip deposited on the sample surface. The metal strip is used as a heater and also as temperature sensor. The sample heating is either transient (transient hot strip method) or modulated (3ω method). The measurements of

* Corresponding author at: INSA de Lyon, Lyon F-69621, France.
Tel.: +33 472 438 183.
E-mail addresses: ali.assy@insa-lyon.fr, aliassy01@gmail.com (A. Assy).

0026-2692/$ - see front matter © 2013 Elsevier Ltd. All rights reserved.
http://dx.doi.org/10.1016/j.mejo.2013.08.006

the heater temperature are coupled with heat transport modeling. Through these measurements, the sample thermal properties are estimated. The uncertainty in the estimations depends then on the parameters used in the thermal modeling of the experiment. Parameters such as contact resistance between the heating strip and the sample, the design and dimensions of the metal strip and substrate can in particular play a major role and have to be taken into account [11,14]. However, characterization of the thermal conductivity of thin films requires certain adaptation of the methods. Using these methods, sufficient heat should pass through the sample for an adequate study of the thermal properties of the sample and a simplified interpretation using straightforward analytical approaches. To address these issues, solutions include adjustment of the sample geometry or fabrication of sophisticated and delicate suspended structures. Moreover, transient methods such as the membrane method have been developed [15,16]. As the method used in this work, this technique includes separate heater and temperature sensors and has been developed for the identification of the in-plane thermal conductivity of thin films [15,16].

Despite their large applicability, all the methods given above need a particular heavy conditioning of set-ups for measurements at different levels of temperature above ambient [7,15,17–19]. Moreover, they need specific apparatus for these measurements. Based on the principle of the membrane method, this paper approach demonstrates the successful extraction of thermal properties of highly diffusive bulk materials above ambient using only a set of microresistors. Quite simple, it can easily be implemented by other investigators.

Section 2 is dedicated to present the method. Section 3 describes the sample under test and the different steps of fabrication. To prove the method applicability, the case of a sample of pure silicon has been chosen. The numerical simulations used to design the samples and to estimate the uncertainty in the thermal parameters determination are given in Section 4. Section 5 describes the different parts of the experimental set-up with their functionality. Our experimental results are analyzed and compared with data found in the scientific literature. Finally, we conclude and give the perspectives of this work.

2. Method used

2.1. Principle

For the experiments, the material to be studied is shaped in a flat suspended film. As shown in Fig. 1, an array of parallel and long resistive wires is deposited on the surface of the sample. One of the resistive wires is heated with an alternating current I of magnitude I_{ac} at angular frequency $\omega=2\pi f$. The power P dissipated in this wire may be written as

$$P = R.I^2 = R.I_{ac}^2/2 + R.I_{ac}^2/2.\cos(2\omega t) \quad (1)$$

where R is the electrical resistance of the heated wire.

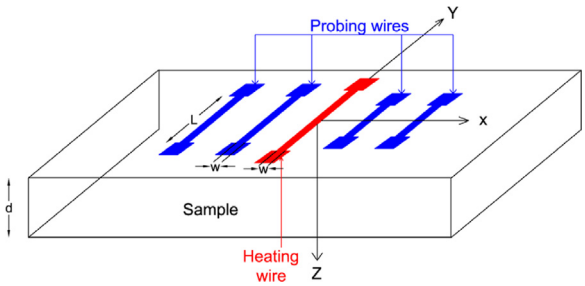

Fig. 1. Schematic of the implemented sample. (For interpretation of the references to color in this figure, the reader is referred to the web version of this article.)

In the material, conductive diffusion of this heating produces a continuous temperature variation called ΔT_{DC} and alternating temperature oscillations at angular frequency 2ω called $\Delta T_{2\omega}$. The length of all the wires is chosen large so that they may be assumed isothermal along their length (in the Y direction in Fig. 1). However, the probing wires are shorter than the heating wire to detect mainly the lateral heat spreading from the heating wire.

By measuring the electrical resistance change of the probing wires $\Delta R_{2w}(x)$, the surface temperature $\Delta T_{2\omega}(x)$ is detected

$$\Delta R_{2\omega}(x) = R_0(x)\beta\Delta T_{2\omega} \quad (2)$$

here $|x|$ is the distance from the heating wire, $R_0(x)$ is the electrical resistance of the probing wire at ambient temperature T_a and β is the temperature coefficient of the electrical resistivity. A direct current i_0 of small magnitude is generated through the probing wires for the $\Delta R_{2\omega}(x)$ measurements. Using a lock-in amplifier, the second harmonic voltage at the probing wires is measured

$$\Delta V_{2\omega}(x) = \Delta R_{2\omega}(x) i_0 = R_0(x)\beta\Delta T_{2\omega}(x) i_0 \quad (3)$$

By measuring the $\Delta T(x)$ dependence on the modulation frequency $F=2f$ and on the distance $|x|$, the sample thermal properties are determined.

2.2. Modeling

The thermal diffusivity of the sample α is given by

$$\alpha = \lambda/(\rho_0 C) \quad (4)$$

where λ, ρ_0, and C are the sample thermal conductivity, density, and heat capacity respectively. The thermal diffusion length μ in the sample material is given by

$$\mu = (\alpha/(2\pi f))^{1/2} \quad (5)$$

Identifying α is all the easier as μ is large compared with the thickness d of the suspended film. This condition is verified while working at small frequencies. In this case, the thermal gradient in the sample thickness may be assumed null (in the Z direction). Moreover, d is chosen so the Biot number defined as $Bi=hd/k$ is much less than 0.1, where h is the convective heat transfer coefficient.

With the fact of $\mu \gg 2\pi w$ where w is the width of the wire, the heating wire is considered punctual. From the resolution of the heat transfer equation, the second harmonic temperature decay measured along a distance x from the heater may then be written as

$$\Delta T_{2\omega}(x) = A\exp(-x/\mu)\exp(-ix/\mu) \quad (6)$$

where

$$A = P/(2dl\lambda)(\alpha/(2\omega))^{1/2} \quad (7)$$

here P is the electrical power dissipated in the heating wire and l is the sample width.

The thermal diffusivity α is deduced from the attenuation of the magnitude $\exp(-x/\mu)$ and the variation of the phase $(-x/\mu)$, both as a function of x. Let α_{am} *and* α_{Φ} the thermal diffusivity extracted from the magnitude attenuation and the phase lag respectively. Then λ could be deduced from A in Eq. (7). By measuring the signal of the probing wires and using Eqs. (3)–(6), the thermal properties of the sample are estimated. This needs a good knowledge of the electrical properties of the material composing the wires. Adjusting the amplitude I_{ac} in the source allows controlling the sample DC temperature at which the thermal properties are identified. Depositing many wires at the sample surface allows the estimation of the DC temperature

$$T_{DCexp} = (1/N)\sum_{i=1}(R(x_i) - R_0(x_i))/(R_0(x_i)\beta) + T_a \quad (8)$$

where N is the number of the probing wires and i is an index for a considered probing wire. A careful design of the sample thickness

and width should guarantee isothermal samples in the DC regime while the measurements in the modulated regime are performed.

3. Description of the sample under test

3.1. The reference material

Because of its well-known thermal properties versus the temperature, we used a sample of pure silicon as reference material. Table 1 gives the values of the thermal properties of silicon determined in literature at different levels of temperature. The value of ρ_0 was determined equal to 2329 kg/m^3 for highly pure silicon at a temperature of 298 K [20]. As the thermal expansion coefficient does not exceed 1% at temperature below 600 K [21], we considered it constant as a function of temperature in our work.

For the test and the method demonstration, a specific sample made of silicon was prepared. Its thickness, width and length were 200 μm, 7 mm and 10 mm respectively. These geometric properties were determined to satisfy the conditions of our model.

3.2. The wire array material

As illustrated in Fig. 1, the heating wire (in red) is located in the middle of the sample surface. The probing wires (in blue) are located on both sides of the heating wire. The main process chosen for fabricating this wires array is photolithography and lift-off. The schematic diagram of the fabrication process flow is shown in Fig. 2.

After a substrate cleaning, a 2 μm-thick nLOF negative photoresist is spun on the silicon wafer. The resist is baked on a hotplate at 110 °C for 1 min. A UV exposure is then carried out (Fig. 2a). A post bake is performed at 110 °C on a hotplate for 1 min. This bake is immediately followed by the resist development in a AZ-351B solution for 60 s, leaving an array of line openings into the resist layer on top of the sample. After the photolithography step, a chromium/gold bilayer, respectively of 50 nm-thick (Cr) and 450 nm thick (Au), is deposited on top of the sample by sputtering (Fig. 2b). The chromium is used as an adhesion layer to stick the gold on silicon. Finally the lift-off step is performed in an acetone bath under ultrasonic excitation (Fig. 2c).

3.3. Characterization of the wires

Table 2 gives the value of the wires section S, electrical resistivity ρ and the coefficient β. Using Atomic Force Microscopy (AFM) in tapping mode, S was measured. Fig. 3 shows an example of the section measurements. As noticed, the wire real section obtained after the process fabrication is uniform but not square as expected. The wires length L is of several millimeters and was measured with optical microscopy. By measuring the wire electrical resistance R by 4-point probes method (4-probe sensing) at ambient temperature, ρ was determined. The chip (sample+wires) was placed in a specific oven and heated to different temperature levels. Then, β was determined from the wire resistance measurements: $R=R_0(1+\beta(T-T_a))$.

Table 1
Thermal properties of pure silicon at different temperature levels.

Temperature (K)	C (J/kg K)[22]	λ (W/m K)[23]	α_{ref} ($\times$10–5 m²/s)[a]	α_{exp} ($\times 10^{-5}$ m²/s)[24]
300	703	148	9.03	8.8
400	760	105	5.93	5.33
500	800	80	4.29	3.8

[a] Data calculated with Eq. (4) and values of k and C from Table 1.

Table 2
Properties of the wires.

Section S (m²)	Electrical resistivity ρ (Ω m) at T_a	Coefficient of temperature β (K^{-1})
$1.66 \pm 0.15 \times 10^{-12}$	$4.15 \pm 0.1 \times 10^{-8}$	$8.8 \pm 0.05 \times 10^{-4}$

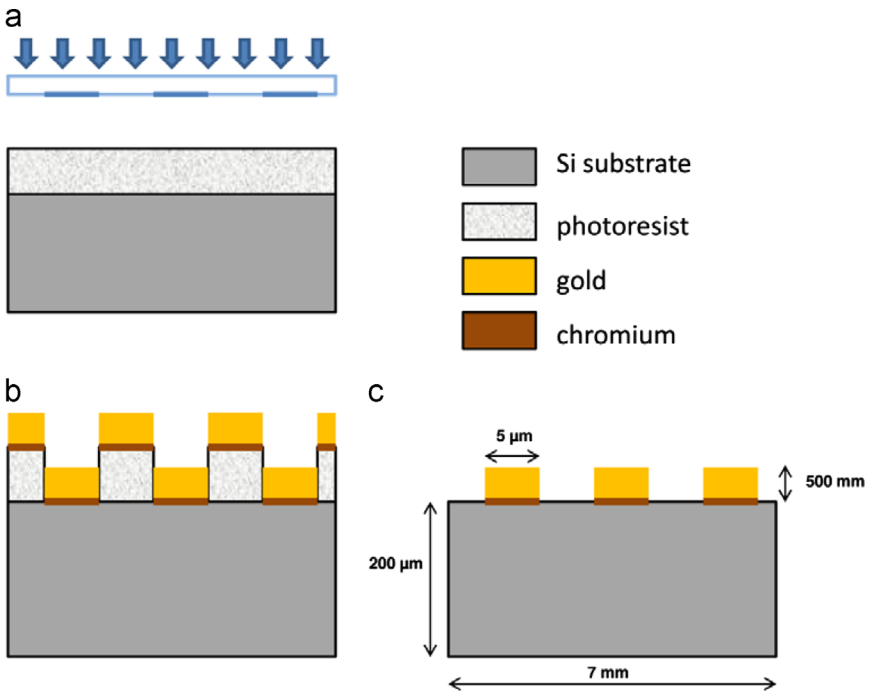

Fig. 2. Process flow for the deposition of the metallic wires array: (a) photolithography; (b) metal deposition; and (c) lift-off process.

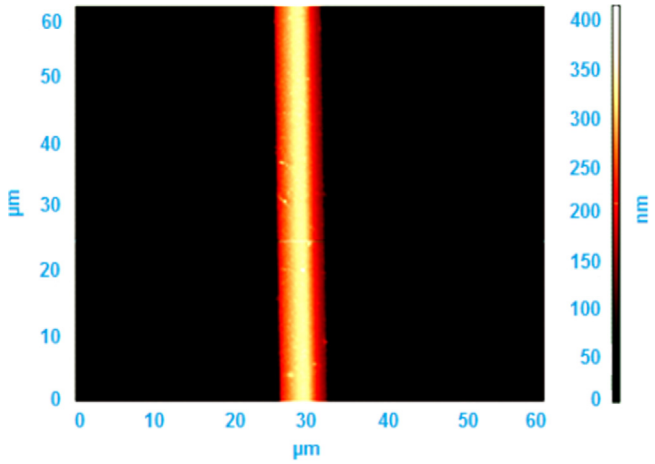

Fig. 3. AFM 2D image of a gold wire. At the top right corner 3D corresponding image.

4. Numerical model and simulation results

Using COMSOL Multiphysics, numerical simulations of the thermal behavior of the Si sample were performed to design the electrical chip. The design includes the determination of the distances between the heating wire and the probing wires as well as the frequency domain where the simple 1D approach is applicable. Assuming in a first approximation that the temperature is uniform along the length of the wires, a 2D model is used.

4.1. Description of the system

As the heating wire is located in the middle at the sample surface, the sample may be assumed symmetric. Using the data of Table 2, a volumetric term of the power P_v is inserted in the section of the heating wire. Thermal losses by natural convection and radiation play an important role on the variation of the sample temperature when the sample is heated to temperatures above T_a. This includes the variation of the two temperature components $\Delta T_{2\omega}$ and T_{DC} as shown in Fig. 4a and b. The emissivity ε of the sample material at a given temperature and the convective heat transfer coefficient h are then required. These two parameters affect directly the determination of the term A in Eq. (6) and then the direct determination of λ.

Since the sample temperature is experimentally determined, this part is just dedicated to the 1D approach validation. Far from the real values, h is supposed equal to $5\,\mathrm{W\,m^{-2}\,K^{-1}}$ and the sample material is here assumed to be a black body.

The interface thermal resistance R_{th} between the wires and the substrate is given by

$$R_{th} = R_{\mathrm{Au/Cr}} + R_{\mathrm{Cr}} + R_{\mathrm{Cr/Si}} \tag{9}$$

where $R_{\mathrm{Au/Cr}}$, R_{Cr} and $R_{\mathrm{Cr/Si}}$ are the thermal resistances at Au/Cr interface, within the Cr layer and at Cr/Si interface respectively. R_{Cr} is equivalent to e/λ_{Cr}, where e is the thickness of the chromium layer and λ_{Cr} is the chromium thermal conductivity. This resistance is about $10^{-10}\,\mathrm{m^2\,K\,W^{-1}}$. $R_{\mathrm{Au/Cr}}$ and $R_{\mathrm{Cr/Si}}$ are dependent on the interface geometry, the materials properties, the process of deposition of the wires on the substrate, etc. However, the values of the thermal resistances found in the scientific literature for metal/semiconductor lie in the range of $10^{-8}\,\mathrm{m^2\,K\,W^{-1}}$. They include the determination of R_{th} at Au/Si interface with transient thermo-reflectance [25,26], with picosecond optical technique [27], and with simulations of molecular dynamics at Si/Au [28] and Si/Pb [29] interfaces. Besides, Gundrum [30] measured R_{th} at Al/Cu interface equal to $0.25\times10^{-9}\,\mathrm{m^2\,K\,W^{-1}}$ using thermo-reflectance.

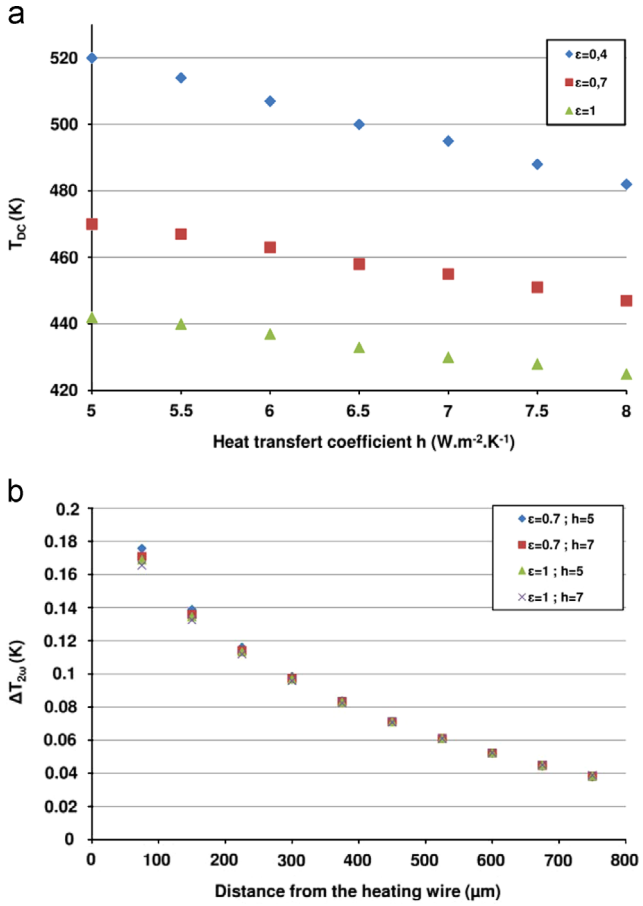

Fig. 4. Effect of the variation of ε and h on the amplitude of the temperature components (a) T_{DC} and (b) $\Delta T_{2\omega}$ (I_{ac}=40 mA, f=40 Hz).

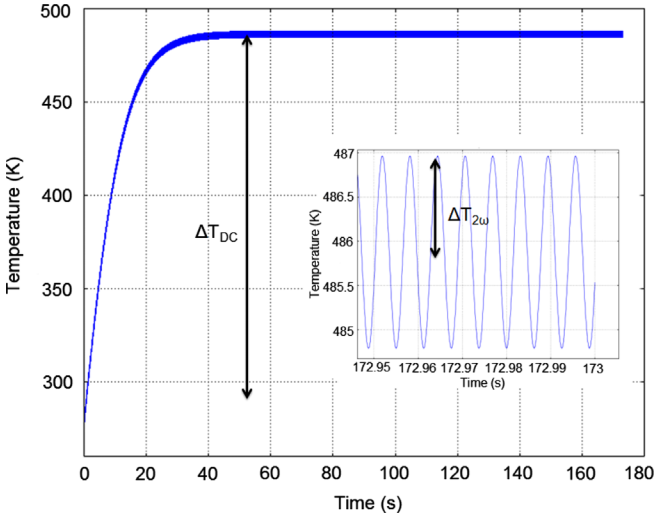

Fig. 5. Variation of the heating wire temperature as a function of time (f=80 Hz).

Then, numerical simulations with values of R_{th} ranging from 0 to $5\times10^{-8}\,\mathrm{m^2\,K\,W^{-1}}$ were performed. The corresponding variation of T_{DC} is almost negligible and lower than 1%. $\Delta T_{2\omega}(x)$ varies with a ratio leaving nevertheless the same exponential variation of $\Delta T_{2\omega}$ as a function of x. As a consequence, the determination of λ through the term A in Eq. (7) requires the determination of R_{th} but α can be determined without this data.

Let us note that the simulations presented in the next part of this section concern the case of perfect contact between the wires and the substrate ($R_{th}=0\ m^2\ K\ W^{-1}$). The thermal properties of silicon (k, d and C) and their dependence on temperature were used for the calculations.

4.2. Simulation results

Heating currents with different magnitudes and different frequencies are used in the simulations. The number of the elements in the mesh is equal to 1300. The time between two steps is at least two hundred times less than the heat power period. The temperature components T_{DC} and $\Delta T_{2\omega}$ were extracted for the wires. Fig. 5 shows the simulated temperature variation versus time at $x=0$ for a frequency of 80 Hz and a magnitude I_{ac} of 60 mA. As the difference in T_{DC} between the heating wire and the furthest probing wire does not exceed 1 K, the sample may be assumed isothermal along x. $\Delta T_{2\omega}$ is three orders of magnitude less than T_{DC}. The very low cut-off frequency of the system, estimated about 5 mHz, justifies this difference.

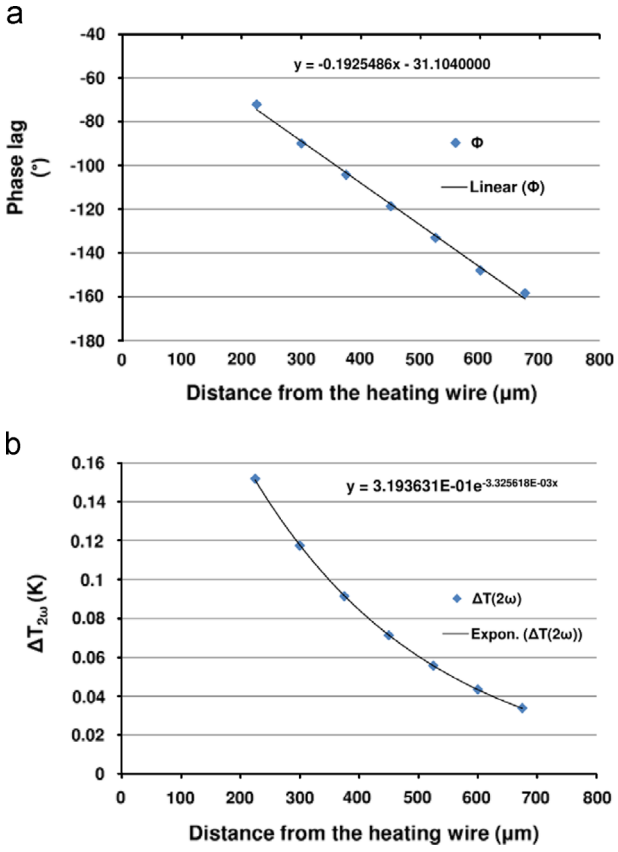

Fig. 6. Simulated variations of (a) the phase lag, (b) $\Delta T_{2\omega}$ as a function of the distance from the heating wire for $I_{ac}=60$ mA and $f=80$ Hz ($\alpha=4.6\times10^{-5}\ m^2\ s^{-1}$ and $\lambda=85\ W\ m^{-1}\ K^{-1}$).

Fig. 6a and b show the magnitude $\Delta T_{2\omega}$ and the phase lag Φ respectively as a function of x. The input values of the thermal properties of the sample are $\alpha=4.6\times10^{-5}\ m^2\ s^{-1}$ and $\lambda=85\ W\ m^{-1}\ K^{-1}$. Using Eq. (6), the thermal properties may be extracted. The distance between the heating wire and the closest probing wire $|x_{min}|$ and the frequency domain were determined. For $|x_{min}|=225\ \mu m$ and $20\le f\le 80$ Hz, the 1D approach is valid and the uncertainty is less than 4%. In fact, the lines of the heat flux become parallel to the sample surface for distances larger than the thickness 200 μm. For distances less than the sample thickness d, the Z part of the heat flux cannot be neglected and as a result the one-dimensional conduction model is not valid anymore, in analogy with the scale analysis showed by Bejan [31]. Considering the identified frequency range, the sample thickness d tends to be smaller than μ when f decreases. When the frequency exceeds 80 Hz, the sample temperature along Z is not uniform anymore and so the 1D model cannot be applicable.

5. Experimental set-up

The experimental set-up is shown in Fig. 7. In this set-up, the AC generator (1) is connected to the current amplifier (2) to generate an alternating current I_{ac} through the heating wire. This wire in red is deposited on the mask (3) and mounted in series with a resistance of 1 KΩ (4). The resistance is linked to an ampere-meter (5) for an accurate measurement of I_{ac}. A DC current generator (6) produces i_0 of small magnitude through the probing wires in yellow. Synchronized with the AC generator, the lock-in amplifier (7) detects the signal $V_{2\omega}$ and the phase lag Φ at the probing wires.

As seen in Fig. 8, two Printed Circuit Boards PCB 1 and PCB 2 are used to integrate the chip into the electrical circuit. Electrical connections link the chip to the BNC plugs at the PCB 1. Each deposited wire on the silicon sample has a number at the PCB 1 plugs. PCB 1 is attached to the PCB 2 by small pins. Bonding wires made of gold of few millimeters in length and 25 μm in diameter connect the pads with PCB 2. As reported by Ji et al. [32], the electrical resistances of the bonding wires and the bond interfaces do

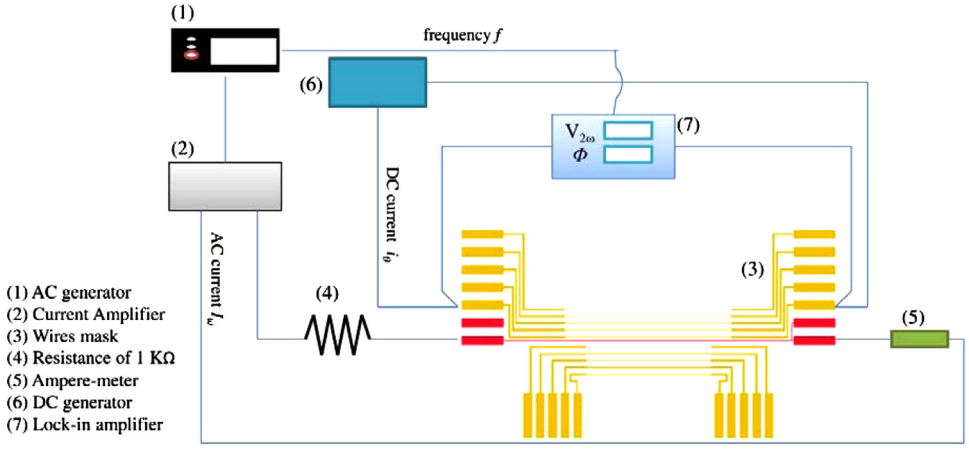

Fig. 7. Schematic of the experimental set-up.

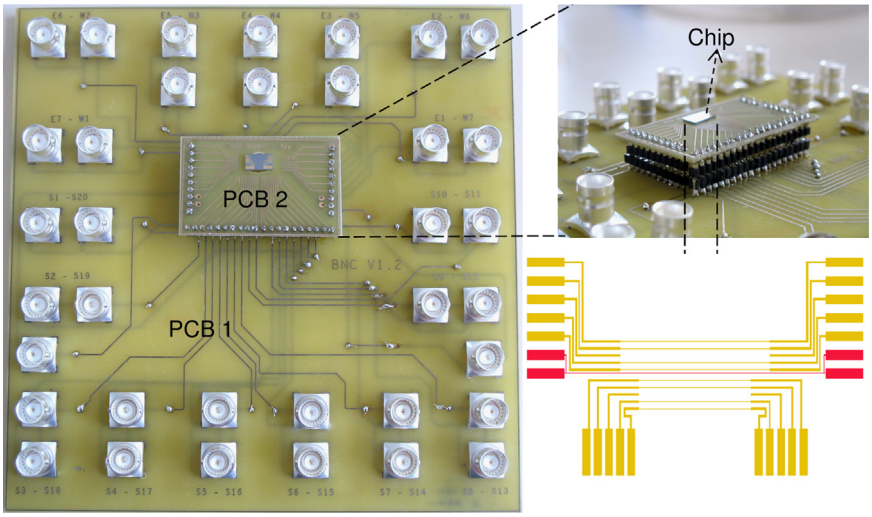

Fig. 8. Electrical connections of the measurements.

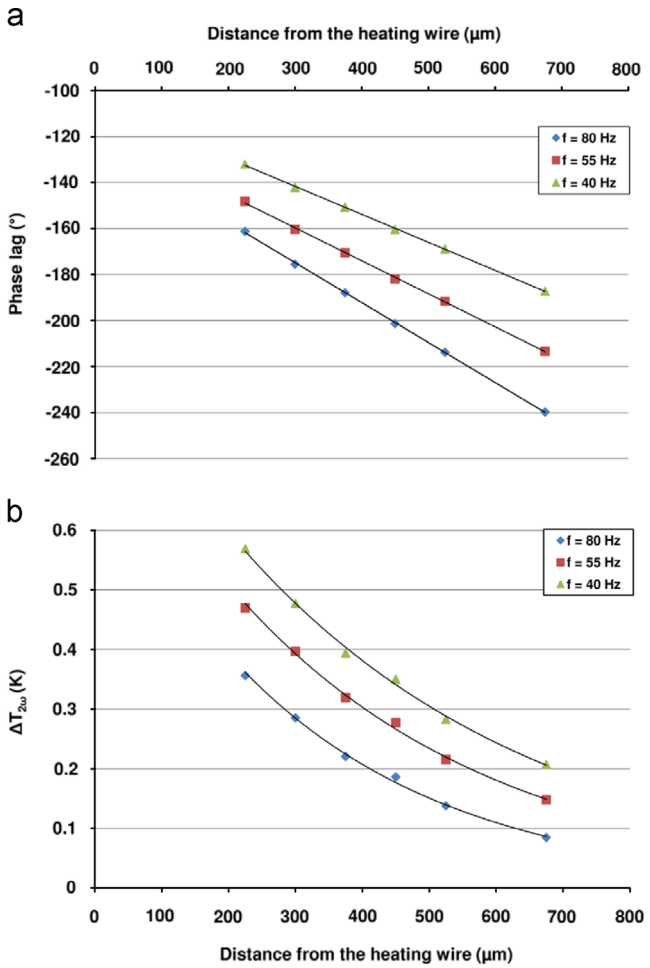

Fig. 9. Experimental variations of (a) the phase lag, (b) $\Delta T_{2\omega}$ as a function of the distance from the heating wire for I_{ac}=60 mA and for different frequencies.

not exceed 100 mΩ. In this work, these resistances are supposed negligible comparing them to those of the wires. Moreover, using a multimeter, it was verified that the electrical resistances of the connection between the PCB 1 and the pins of the PCB 2 are of few milliOhms. Taking all of this into account, it can be said that the electrical resistances measured at the PCB 1 plugs correspond to the wires of the electrical chip.

Table 3
Si thermal diffusivity experimentally determined.

I_{ac} (mA)	α_{am} ($\times 10^{-5}$ m² s^{-1})	α_{Φ} ($\times 10^{-5}$ m² s^{-1})	T_{DCexp} (K)[a]	λ (W m^{-1} K^{-1})
40	6.5 ± 0.5	6.8 ± 0.5	365 ± 5	112 ± 8
60	5 ± 0.1	5.5 ± 0.1	465 ± 5	91 ± 3

[a] Temperature experimentally determined using Eq. (8) at the probing wires.

6. Experimental results

Experiments were performed for frequencies between 20 Hz and 80 Hz. Two different magnitudes I_{ac} of 40 and 60 mA were used to heat the sample. Fig. 9a and b gives an example of the measurements for I_{ac} of 60 mA for three different frequencies: 40, 55, and 80 Hz. For both I_{ac}, the exponential tendency of $\Delta T_{2\omega}$ and the linear tendency of Φ are found as a function of |x|.

Using Eqs. (3) and (6), α_{am} and α_{Φ} were extracted. By fitting the experimental curves with the numerical data, λ should be determined directly. The fitting requires the determination of the heat loss and the interface thermal resistance as discussed before. However, λ can be determined using Eq. (4) and data from Table 1. Table 3 gives the values of the estimated thermal properties of the sample and their corresponding temperatures. Using Eq. (8), the sample temperature T_{DCexp} is determined experimentally. The experimental results obtained are in good agreement with the literature values listed in Table 1.

7. Conclusions and perspectives

This work reports the first step of validation of a simple technique based on adaptation of the membrane method principle in modulated regime to highly diffusive bulk materials. It demonstrates the successful extraction of thermal properties of such a material at different temperatures from ambient to 500 K using only a set of microresistors. Using a simple 1D approach, the technique is valid for a specified frequency range for the case of a silicon sample with an uncertainty estimated less than 4%. The silicon thermal properties values obtained at different temperatures above ambient are promising and are in good agreement with data found in the scientific literature. Quite simple, the technique can easily be implemented by other investigators. Characterizing the thermal properties of another sample material can nevertheless induce the re-dimensioning of the

system (sample thickness, resistive wire dimensions and the distances between the resistive wires).

Performing the measurements with this technique requires a more exact estimation of the uncertainties linked to parameters of influence. They include the emissivity ε of the sample material, the convective heat transfer coefficient h, and the interface thermal resistance between the wires and the sample. Direct measurement of the thermal conductivity should then be also allowed. Characterizing the parameters of influence is part of the perspectives of this work.

The presented method allows estimating the in-plane component of the sample thermal properties. Seeking the thermal characterization of complex materials such as multilayered materials deposited on a silicon substrate, the perspectives of this work are also based on its technical adaptation for such applications. Therefore, a more realistic model is under development to extend the frequency domain of use of the technique.

Acknowledgment

The authors acknowledge financial support from the ANR-07-PNANO-047. We are also pleased to acknowledge the technical contribution of our colleague E. Pané Farré and the SOITEC Company (Grenoble—France) for providing the silicon samples.

References

[1] W. Parker, R. Jenkins, C. Butler, G. Abbott, Flash method of determining thermal diffusivity, heat capacity, and thermal conductivity, Journal of Applied Physics 32 (1961) 1679–1684.
[2] T. Baba, A. Ono, Improvement of the laser flash method to reduce uncertainty in thermal diffusivity measurements, Measurement Science and Technology 12 (2001) 2046.
[3] A. Boccara, D. Fournier, J. Badoz, Thermo-optical spectroscopy: detection by the "mirage effect", Applied Physics Letters 36 (1980) 130–132.
[4] F. Charbonnier, D. Fournier, Compact design for photothermal deflection (mirage): spectroscopy and imaging, Review of Scientific Instruments 57 (1986) 1126–1128.
[5] L. Inglehart, A. Broniatowski, D. Fournier, A. Boccara, F. Lepoutre, Photothermal imaging of copper-decorated grain boundary in silicon, Applied Physics Letters 56 (1990) 1749–1751.
[6] L. Pottier, Micrometer scale visualization of thermal waves by photoreflectance microscopy, Applied Physics Letters 64 (1994) 1618–1619.
[7] D. Rochais, H. Le Houëdec, F. Enguehard, J. Jumel, F. Lepoutre, Microscale thermal characterization at temperatures up to 1000 C by photoreflectance microscopy. Application to the characterization of carbon fibres, Journal of Physics D: Applied Physics 38 (2005) 1498.
[8] A. Rosencwaig, J. Opsal, W.L. Smith, D. Willenborg, Detection of thermal waves through optical reflectance, Applied Physics Letters 46 (1985) 1013–1015.
[9] L. Fabbri, P. Fenici, Three-dimensional photothermal radiometry for the determination of the thermal diffusivity of solids, Review of Scientific Instruments 66 (1995) 3593–3600.
[10] B. Rémy, A. Degiovanni, D. Maillet, Measurement of the in-plane thermal diffusivity of materials by infrared thermography, International Journal of Thermophysics 26 (2005) 493–505.
[11] T. Borca-Tasciuc, G. Chen, Experimental techniques for thin-film thermal conductivity characterization, Thermal Conductivity: Theory, Properties, and Applications (Section 2), Springer (2004) 205–237.
[12] S.E. Gustafsson, E. Karawacki, Transient hot-strip probe for measuring thermal properties of insulating solids and liquids, Review of Scientific Instruments 54 (1983) 744–747.
[13] D.G. Cahill, Thermal conductivity measurement from 30 to 750 K: the 3ω method, Review of Scientific Instruments 61 (1990) 802–808.
[14] H. Wang, M. Sen, Analysis of the 3-omega method for thermal conductivity measurement, International Journal of Heat and Mass Transfer 52 (2009) 2102–2109.
[15] X. Zhang, C.P. Grigoropoulos, Thermal conductivity and diffusivity of free-standing silicon nitride thin films, Review of Scientific Instruments 66 (1995) 1115–1120.
[16] A. Jacquot, G. Chen, H. Scherrer, A. Dauscher, B. Lenoir, Improvements of on-membrane method for thin film thermal conductivity and emissivity measurements, Sensors and Actuators A: Physical 117 (2005) 203–210.
[17] T. Baba, A. Ono, Improvement of the laser flash method to reduce uncertainty in thermal diffusivity measurements, Measurement Science and Technology 12 (2001) 2046.
[18] A. Jain, K.E. Goodson, Measurement of the thermal conductivity and heat capacity of freestanding shape memory thin films using the 3ω method, Journal of Heat Transfer 130 (2008) 102402.
[19] J. Cabrero, F. Audubert, R. Pailler, A. Kusiak, J. Battaglia, P. Weisbecker, Thermal conductivity of SiC after heavy ions irradiation, Journal of Nuclear Materials 396 (2010) 202–207.
[20] A. Smakula, V. Sils, Precision density determination of large single crystals by hydrostatic weighing, Physical Review 99 (1955) 1744–1746.
[21] H. Watanabe, N. Yamada, M. Okaji, Linear thermal expansion coefficient of silicon from 293 to 1000 K, International Journal of Thermophysics 25 (2004) 221–236.
[22] G. Chen, Thermal conductivity and ballistic-phonon transport in the cross-plane direction of superlattices, Physical Review B 57 (1998) 14958.
[23] C. Glassbrenner, G.A. Slack, Thermal conductivity of silicon and germanium from 3 K to the melting point, Physical Review 134 (1964) A1058.
[24] H. Shanks, P. Maycock, P. Sidles, G. Danielson, Thermal conductivity of silicon from 300 to 1400 K, Physical Review 130 (1963) 1743.
[25] P.L. Komarov, M.G. Burzo, G. Kaytaz, P.E. Raad, Transient thermo-reflectance measurements of the thermal conductivity and interface resistance of metallized natural and isotopically-pure silicon, Microelectronics Journal 34 (2003) 1115–1118.
[26] A.N. Smith, J.L. Hostetler, P.M. Norris, Thermal boundary resistance measurements using a transient thermoreflectance technique, Microscale Thermophysical Engineering 4 (2000) 51–60.
[27] R. Stoner, H. Maris, Kapitza conductance and heat flow between solids at temperatures from 50 to 300 K, Physical Review B 48 (1993) 16373.
[28] C.A. Da Cruz, P. Chantrenne, X. Kleber, Molecular dynamics simulations and Kapitza conductance prediction of Si/Au systems using the new full 2NN MEAM Si/Au cross-potential, Journal of Heat Transfer 134 (2012) 062402.1–062402.8.
[29] K. Termentzidis, J. Parasuraman, C.A. Da Cruz, S. Merabia, D. Angelescu, F. Marty, T. Bourouina, X. Kleber, P. Chantrenne, P. Basset, Thermal conductivity and thermal boundary resistance of nanostructures, Nanoscale Research Letters 6 (2011) 1–10.
[30] B.C. Gundrum, D.G. Cahill, R.S. Averback, Thermal conductance of metal–metal interfaces, Physical Review B 72 (2005) 245426.
[31] A. Bejan, Heat Transfer, John Wiley & Sons, New York (1993) vol. 1971.
[32] H. Ji, M. Li, C. Wang, H.S. Bang, In situ measurement of bond resistance varying with process parameters during ultrasonic wedge bonding, Journal of Materials Processing Technology 209 (2009) 139–144.